CircRNA_0000927 promotes inflammatory response to neuronal injury via miR-126a-5p/PGC-1α axis in acute ischemic stroke

Meng Wang
First Teaching Hospital of Tianjin University of Traditional Chinese Medicine
Hong Li
First Teaching Hospital of Tianjin University of Traditional Chinese Medicine
Yulin Qian
First Teaching Hospital of Tianjin University of Traditional Chinese Medicine
Shanshan Zhao
First Teaching Hospital of Tianjin University of Traditional Chinese Medicine
Hao Wang
First Teaching Hospital of Tianjin University of Traditional Chinese Medicine
Yu Wang
First Teaching Hospital of Tianjin University of Traditional Chinese Medicine
Tao Yu (nkutongleishi@163.com)
First Teaching Hospital of Tianjin University of Traditional Chinese Medicine

Research Article

Keywords: AIS, CircRNA_0000927, miR-126a-5p, PGC-1α, inflammatory response, neuronal injury

Posted Date: December 1st, 2022

DOI: https://doi.org/10.21203/rs.3.rs-2307258/v1

Abstract

Purpose

We investigated the role of CircRNA_0000927 on the occurrence and development of acute ischemic stroke (AIS) and neuronal injury by targeting the miR-126a-5p/PGC-1α axis to find a novel clinical drug target and prediction and treatment of AIS.

Methods

The mouse AIS animal model was used *in vivo* experiments and hypoxia/reoxygenation cell model *in vitro* was established. Firstly, infarction volume and pathological changes of mouse hippocampal neurons were detected using HE staining. Secondly, rat primary neuron apoptosis was detected by flow cytometry assay. The numbers of neuron, microglia and astrocytes were detected using immunofluorescence (IF). Furthermore, binding detection was performed by bioinformatics database and double luciferase reporter assay. CircRNA_0000927 localization was performed using fluorescence in situ hybridization (FISH). CircRNA_0000927, miR-126a-5p and PGC-1α mRNA expression was performed using RT-qPCR. NLRP3, ASC, Caspase-1 and PGC-1α protein expression was performed using Western blotting. IL-1β was detected by ELISA assay.

Results

Mouse four-vessel occlusion could easily establish the animal model, and AIS animal model had an obvious time-dependence. HE staining showed that, compared with the sham group, infarction volume and pathological changes of mouse hippocampal neurons were deteriorated in the model group. Furthermore, compared with the sham group, neurons were significantly reduced, while microglia and astrocytes were significantly activated. Moreover, the bioinformatics prediction and detection of double luciferase reporter confirmed the binding site of circRNA_0000927 to miR-126a-5p and miR-126a-5p to PGC-1α. CircRNA_0000927 and PGC-1α expression was significantly down-regulated and miR-126a-5p expression was significantly up-regulated in AIS animal model *in vivo*. At the same time, the expression of inflammasome NLRP3, ASC, Caspase-1 and pro-inflammatory factor IL-1β was significantly up-regulated *in vivo* and *in vitro.* The over-expression of circRNA_0000927 and miR-126a-5p inhibitor could inhibit the neuron apoptosis and the expression of inflammasome NLRP3, ASC, Caspase-1 and pro-inflammatory factor IL-1β and up-regulate the expression of PGC-1α *in vitro*. Finally, over-expression of circRNA_0000927 and miR-126a-5p inhibitor transfected cell model was significant in relieving the AIS and neuronal injury.

Conclusion

CircRNA_0000927 promotes inflammatory response to neuronal injury via miR-126a-5p/PGC-1α axis in AIS.

1. Introduction

Acute ischemic stroke (AIS) is one of the most common cerebrovascular diseases, leading to severe disability and mortality. According to clinical statistics, AIS is accounting for about 87% of all cerebrovascular diseases. Neuronal death, neuro-inflammation and destruction of neurovascular units caused by AIS lead to severe neurological symptoms (Guida et al., 2019). Timely restoration of cerebral blood flow perfusion and neuro-protective treatment are the main goals of AIS treatment. Unfortunately, effective treatments for AIS are limited and only intravenous thrombolytic therapy is recognized as an effective treatment. However, the time window for intravenous thrombolysis is relatively narrow, and 4.5 h after AIS is considered as the effective time window in many countries, including China (Brancaccio et al., 2022). Many clinical trials have reported that effective blood flow reperfusion can reduce acute ischemic brain injury and improve the clinical prognosis of patients with AIS (Hellwig et al., 2022; Rog-Zielinska et al., 2015). At present, in addition to intravenous thrombolytic therapy as the first-line treatment, intra-arterial thrombolytic therapy can be used for patients with a time window of 4.5 h or less than 6 h (Miozzo et al., 2022; Yao and Vanduffel, 2022). In a study published in the New England Journal of Medicine in 2018, Nogueira et al. suggested that mechanical thrombectomy could be used in patients with AIS onset longer than 6 h and less than 24 h (Choi et al., 2020; Rog-Zielinska et al., 2015). In addition to vascular reperfusion therapy, clinical also includes antiplatelet aggregation therapy, statin therapy, blood pressure and blood glucose management, brain edema and other conventional treatment measures (Chaube et al., 2015; Tarocco et al., 2022). Although many treatment measures have been developed for AIS, the benefits of timely reperfusion have been understood and thrombolytic therapy has become the basis of the current treatment of AIS, unfortunately, the effective treatment and clinical benefits of AIS are still not optimistic.

Over the past few decades, our understanding of the pathophysiology of AIS has progressed considerably, but the mechanisms by which neuro-inflammatory responses aggravate neuronal ischemia-reperfusion injury are still not fully elucidated (Miozzo et al., 2022). Immune and inflammatory responses are considered to be the key factors involved in the pathophysiology of AIS, which are closely related to the complex pathological changes of AIS (Rog-Zielinska et al., 2015; Wu et al., 2015). The inflammatory response occurs very rapidly within hours after stroke, and activation of neuro-immunity can directly affect the initiation, proliferation, and recovery stages of ischemic brain injury (Nichols et al., 2018). Therefore, the inflammatory signaling pathways run through all stages of stroke, from the brain injury stage caused by ischemia in the early stage to the regenerative process of tissue repair in the later stage of stroke (Yang et al., 2022c).

The specific mechanisms of inflammatory injury in stroke include: cerebral ischemia induces a large number of activation of innate glial cells (mainly microglia and astrocytes) in the central nervous system (CNS), and a variety of pro-inflammatory factors, such as IL-1β, IL-6 and TNF-α, released by glial cells

directly aggravate the nerve injury (Yang et al., 2022b; Yoshida and Ohki, 2020). Brain ischemia directly induces the destruction of the blood-brain barrier (BBB), leading to the infiltration of peripheral immune cells (Wu et al., 2015). In addition, the inflammatory factors secreted by glial cells further aggravate the permeability of BBB and the infiltration of peripheral immune cells, and the inflammatory factors secreted by infiltrating immune cells aggravate the nerve injury (Zhang et al., 2019). Infiltrating peripheral immune cells interact with central innate glial cells to proliferate and differentiate in situ, amplifying local inflammatory response and further aggravating the ischemic brain injury (Zhang et al., 2019; Zhu et al., 2019). Many studies have suggested that the promotion of inflammation in the CNS could enlarge the area of cerebral infarction and aggravate the neurological injury in animal models of AIS (Yoshida and Ohki, 2020; Zemel et al., 2021). Therefore, for the treatment of AIS, intervention of the inflammatory response in the CNS can be regarded as a feasible alternative treatment.
In recent years, circRNA has got widely attention and research from many aspects in biomedical field. In the study of many diseases, some circRNAs with functions of diagnosis and prognosis have gradually emerged (Liang et al., 2022; Presslauer et al., 2017). Recent findings have also confirmed that circRNA has a variety of biological functions, including regulating the chromosome recombination, controlling the gene transcription, pre-transcription mRNA processing, and affecting the protein signal function and localization (Liang et al., 2022). CircRNAs involved in stroke also have a wide range of mechanisms, including DNA inactivation, methylation, transcriptional promotion, activation of other RNA molecules, and so on (Bauer et al., 2022; Meng et al., 2022). Moreover, scientists have found that circRNA can undergo various epigenetic modifications, including methylation and ubiquitination, and act as ceRNA with some microRNAs (miRNAs) to form a regulatory network (Siegerist et al., 2021).

CircRNA_0000927 is a hot star molecule in recent years. It is expressed in many normal tissues and the expression level is also strictly regulated, which is extremely important for embryo development, organism growth and development (Song et al., 2017). However, circRNA_0000927 is mostly absent due to gene deletion and hypermethylation in the regulatory region and other reasons, and is involved in the occurrence of diseases. In many types of cerebrovascular diseases, circRNA_0000927 can play a role in occurrence and development of cerebrovascular diseases (Song et al., 2021). However, unfortunately, the role of circRNA_0000927 in AIS has not yet been revealed.

In recent years, more and more studies have shown that miRNA expression disorders exist in a variety of cerebrovascular diseases such as AIS, and it is closely related to the diagnosis, stage, progression, prognosis and treatment response of cerebrovascular diseases, suggesting that miRNA may be involved in every process of cerebrovascular disease occurrence and development (Xu et al., 2022; Zhang et al., 2021). Multiple studies have reported that the expression of miR-126a-5p is up-regulated in cerebral palsy, cerebral blood clot and Alzheimer's disease (Yang et al., 2022a). However, at present, the relationship between miR-126a-5p and AIS is not clear, and no studies have been reported at home and abroad.

Peroxisome proliferator-activated receptor-γ co-activator-1α (PGC-1α), as a major co-transcriptional regulator, co-regulates the expression of genes related to mitochondrial biosynthesis by interacting with many transcription factors (Baldelli et al., 2014). At the same time, linear correlation analysis showed that

the decreased level of PGC-1α was directly proportional to the number of neurons. It was speculated that the possible mechanism was that the decreased level of mitochondrial antioxidant components and uncoupling proteins caused by the decreased level of PGC-1α, which eventually led to the loss of neurons and neuro-degeneration (De Vitto et al., 2019). In addition, over-expression of PGC-1α in human primary astrocytes significantly inhibited the oxidative stress damage and pro-inflammatory factor production (Savini et al., 2022). In conclusion, increasing the level of PGC-1α in neurons can produce significant neuro-protective effects. However, the effect of increasing PGC-1α in neurons on AIS and specific molecular mechanism are still unclear. Therefore, a better description of the mechanism of PGC-1α is of great significance for the treatment of AIS.

In this study, we predicted the relationship between circRNA_0000927 and miR-126a-5p, or miR-126a-5p and PGC-1α in AIS by bioinformatics database. Furthermore, the correlation between the function and regulatory of AIS and the expression level of circRNA_0000927, miR-126a-5p and PGC-1α were further analyzed. Finally, experiments related to cell and animal models were established to study the role of circRNA_0000927, miR-126a-5p and PGC-1α in AIS, and to determine the target genes and related mechanism. In order to find more effective clinical prediction and treatment of AIS to provide the clinical basis and new treatment targets.

2. Materials And Methods

Animal model establishment and grouping

In this study, SPF C57BL/6J mice (20-23g, purchased from Beijing Vital River Laboratory Animal Technology Co., Ltd., China) were fed in SPF environmental conditions of half day light and half day dark, temperature was 22 ± 2°C and humidity was 60%±10%. C57BL/6J mice were randomly divided into sham and model groups. Global cerebral ischemia stroke model was prepared by four-vessel occlusion (Chaube et al., 2015): bilateral common carotid arteries were separated by a midneck incision after rats anesthesia, and the first transverse pterygous foramen was exposed in the posterior occipital position. The passing vertebral arteries under the first transverse pterygous foramen were thermo-coagulated for 2-4s for permanent occlusion. 24 h later, both common carotid arteries were clipped for 20 min under the awake state of the mice, and then permanent perfusion was performed. The criteria for the success of the animal model was as follows: the mice were in coma within 30-60s of ischemia, bilateral pupil dilation, and the righting reflex disappeared. In sham group, only blood vessel isolation and exposure were performed, without vertebral artery electrocoagulation and common carotid artery clipping.

Brain tissues were collected at 1, 3 and 7 days after modeling and a portion of the brain tissues was placed in 4% paraformaldehyde (PFA) and the rest was frozen in liquid nitrogen and stored at -80°C in preparation for subsequent experiments. The experimental mice followed the regulations of the Experimental Animal Ethics Committee of the Ministry of Science and Technology and the Laboratory Management Regulations of the Animal Center of the Institute of Radiation Medicine, Chinese Academy of Medical Sciences.

Isolation and culture of primary neurons

The mice were sterilized by 75% alcohol and then the brain tissues were slowly removed on a clean hood, and the cerebellum, brainstem, dura mater, pia mater and blood vessels were removed on ice. Transfering the remaining brain tissues to a petri dish that had been added with Hank's buffer, and cut up the brain tissues. After Hank's buffer was removed by pipetting, 3 mL trypsin was added and digested in cell incubator for 10 min. The samples were blew gently and added 1 mL DNase to tissue digestion. The tissue digestion was terminated by adding 3 mL DMEM complete medium. For the isolation and culture of primary neurons, the resuspended cells were added to poly-lysine coated petri dishes containing high glucose DMEM medium and incubated in the 37℃ incubator for 4h. The high glucose DMEM medium was removed, neurobasal medium containing 2% B27, 1% glutamic acid, 1% HEPES and 1% penicillin/streptomycin was added and cultured in the 37℃ incubator. The neurobasal medium was replaced every three days and cultured for 7–10 days to obtain the primary neurons.

Cell culture

The primary neurons were cultured in neurobasal medium (Solarbio, China) supplemented with 10% fetal bovine serum (FBS, Hyclone, USA) in a 37℃ incubator.

Cell transfection

All the plasmids (vector-miR-126a-5p inhibitor and vector-circRNA_0000927 over-expression) were purchased from Sangon Biotech. Co., Ltd. (Shanghai, China). The cells were transfected by lipo3000 (Biosharp, China) according to the manufacturer’s protocol. 24-48h later, cells were used to transfection-efficiency testing via RT-qPCR.

Hypoxia/reoxygenation cell model

The mouse neuronal injury was simulated by neuron hypoxia/reoxygenation. According to the adjustment of the preliminary experimental results, the time of hypoxia was determined for 3h and the time of reoxygenation for 24h, and the process of primary neurons injury *in vitro* was successfully simulated. The complete DMEM medium was replaced with FBS-free and glucose-free DMEM medium. Then, the cells were placed in an anaerobic producing airbag containing an oxygen indicator, and the bag was filled with mixed gas until the oxygen indicator turned pink. The bag was sealed and placed in an incubator for hypoxia 3h. After the end of hypoxia, the culture plate was removed from the anaerobic airbag and the medium was updated. The high-glucose DMEM medium containing 10% FBS was replaced and reoxygenated in a normal incubator for 24h to simulate the injury of primary neurons *in vitro.*

Flow cytometry

The primary neurons were collected with adjusting the cell density of 1×10^6 cells/mL. Then the cells were washed with PBS two times and centrifugal collected 5×10^5 cells. Next, the cells were resuspended by

500μLbinding buffer and 5μL Annexin V-FITC was added and mixed. Finally, 5μLPropidium Iodide was added and mixed at room temperature and reacted for 15 min in dark. Flow cytometry was used to detect and analyze the proportion of cell apoptosis. The above experiment was repeated for three times and recorded the data.

Histopathological examination

For Hematoxylin-eosin (HE) staining, the mouse brain tissues were fixed with 4% PFA, dehydrated in gradient ethanol, soaked in xylene, embedded in paraffin, dewaxed wirh xylene and gradient ethanol successively and sectioned. The thickness of the sections was about 3μm. The slices were sealed with permount TM mounting medium (Genink, Tianjing China,), observed and photographed using a microscope (Olympus BX51, Japan).

Immunofluorescence (IF)

For immunofluorescence, FITC labeled fluorescent primary antibodies Iba-1 (Affinity, USA, dilution:1:200), GFAP (CST, USA, dilution:1:200) and NeuN (CST, USA, dilution:1:200) were incubated overnight at 4°C. On the next day, sections were rewarmed, washed with PBS, anti-rabbit IgG (H + L) Alexa Fluor® 488 Conjugate secondary antibody (CST, USA, dilution:1:500) was incubated in dark for 1h. After restaining with DAPI, the slices were observed by fluorescence microscope (OLYMPUS, Japan, BX51) and photographed.

Fluorescence in situ hybridization (FISH)

The mouse brian tissues were fixed with fresh formaldehyde (1–4%) for 1-2h at room temperature, centrifuged at 12000g for 5min, poured off the supernatant and resuspend the samples with 1xPBS (pH 7.6). The samples were stored in a 1:1 mix of PBS/ethanol at -80°C until further processing. For the hybridization mixtures, adding 1 volume of probe working solution (50 ng.μL^{-1} DNA) to 9 volume of hybridization buffer in a 0.5-mL microfuge tube and keeping the probe working solution dark and on ice. Hybridization vessels were prepared from 50 mL polyethylene tubes, inserted a piece of blotting paper into a polyethylene tube and soaked it with the remaining hybridization buffer. 10 μL hybridization mix was added to the samples in each well and place the slide into the polyethylene tube (in a horizontal position) and incubated at 46°C for at least 90 min. The slices were quickly rinsed carefully with a bit of washing buffer, transfered slices into preheated washing buffer and incubated for 25 min at 48°C. Then the slices were rinsed with distilled H_2O and counterstained with 10 μL DAPI solution, and incubated for 3 min. Finally, the slices were sealed with permount TM mounting medium (Genink, Tianjing China), observed and photographed using a microscope (Olympus BX51, Japan).

ELISA assay

The mouse fresh brain tissues and cell samples were added to PBS buffer (Solarbio, China) and ground using a high-throughput tissue homogenizer (Techin TJ-800D, China). The homogenate was centrifuged

at 10000×g for 5min, and the supernatant was collected. The BCA protein detection kit (Beijing Solarbio Biotechnology Co., Ltd., China) was used for protein quantification. The concentrations of IL-1β (Cloud-Clone, USA) was detected by ELISA kit. The ELISA kit was detected according to the kits instruction.

Western blotting

The mouse fresh brain tissues and cell samples were ground and lysed in RIPA buffer (Solarbio, China). After tissues or cell samples lysis, the samples were centrifuged at 12000rpm for 10min at 4℃ and supernatants were obtained. The protein concentration was determined using the BCA kit (Solarbio, China). The proteins were denatured by boiling water, and the samples were loaded for SDS-PAGE gel electrophoresis. After electrophoresis, the proteins were transferred to PVDF membrane (Millipore, USA), and the condition was 250mA constant flow for 1.5h. Samples were blocked with 5% non-fat milk solution for 1 h and then probed with primary antibodies PGC-1α (1:1000, Abcam, USA) NLRP3 (1:1000, Abcam, USA) ASC (1:1000, Affinity, USA) and Caspase-1 (1:1000, Abcam, USA) for shaking incubation at 4℃ overnight. After 1×TBST buffer washing for three times, secondary antibody was used for detection included HRP-conjugated anti-rabbit IgG (1:3000, Bioss, China). The samples were incubated for 1 h at room temperature and washed three times with 1×TBST, and incubated with ECL kit (Solarbio, China) for 2min at room temperature for color development. After ECL kit detection, the automatic chemiluminescence image analysis system (Tanon, China) was used for scanning imaging and taking photos. The software Gelpro32 (Tanon, China) was used to analyze the gray values.

RT-qPCR

The Trizol reagent (Invitrogen, USA) was used for total RNA of fresh brain tissues and cell samples extraction. The purity and concentration of RNA were detected by NanoDrop and the operation process was performed in strict accordance with the kit operation instructions. The RNA reverse transcription was performed using Revertaid First Strand cDNA Synthesis Kit (Thermo, USA). RT-qPCR was performed using SYBR®Green Kit (TaKaRa, Japan) with GAPDH as the reference gene. The Applied Biosystems Step One Plus Real-Time PCR system (Thermo, USA) was used for Ct values detection. Relative expression of target genes was analyzed using Ct values and $2^{-\triangle\triangle Ct}$ values. The primers used in this study were synthesized by BGI (China), and the primer sequences are shown in Table 1.

Table 1
Primers used in this study

Gene name		Sequences (5'-3')	Size(bp)
CircRNA_0000927	F	TTAGGCAGGTGGGAGATGATG	81
	R	CTGCAATTATTAAATGCTCATCACTG	
miR-126a-5p	F	CGCCATTATTACTTTTGGTACGCG	
PGC-1α	F	CTGGGTGGATTGAAGTGGTGTAG	75
	R	TATGTTCGCAGGCTCATTGTTGT	
GAPDH	F	GGTGGACCTCATGGCCTACA	82
	R	CTCTCTTGCTCTCAGTATCCTTGCT	
U6	F	CTCGCTTCGGCAGCACA	94
	R	AACGCTTCACGAATTTGCGT	

Double luciferase assay

The binding sites between miR-126a-5p and PGC-1α mRNA and circRNA_0000927 and miR-126a-5p were predicted basing bioinformatics database. The deionized water was diluted the 5×PLB before use. Added 50 μL of diluted 1×PLB to each well and shaked on a shaker for 30 min. The 24-well microplate was added with 50 μL of supernatant to each well, and 500 μL of Luciferase Assay Reagent (Boster, China) premixed was added. After the measurement was completed, 450 μL of stop reagent premixed was added to each well and allowed to stand for 5 s, and then the data was measured to determine the intensity of the luciferase reaction. Finally, the results were calculated the ratio of the two sets of data.

Statistical analysis

The classic scientific software SPSS 24.0 (IBM, USA) was used for data statistical analysis. The data were expressed as mean ± standard deviation.The *t*-test was used for comparison between the two groups and one-way ANOVA analysis of variance was used among the multiple groups. $P < 0.05$ was considered statistically significant. The analyzed data were plotted using GraphPad Prism 7.0 software (La Jolla, USA).

3. Results

The animal model of AIS is successfully established

In order to confirm the success of the AIS animal model, TTC and HE staining were performed on the brain tissues of mice. TTC staining was used to evaluate the infarction area of mice at 1, 3 and 7 days

after stroke and the results showed that the infarction area had time-dependent changes with an increase at 1 day after stroke and a gradual decrease at 3 and 7 days after stroke (**data not shown**). Furthermore, HE staining showed that mouse hippocampus neuron structure was complete and cytoplasmic staining was uniform in the sham group and the pathological changes of rat hippocampal neurons in the model group were obviously, the nuclei were pycnosis, remarkable rupture and interstitial edema at 1 day after stroke and the extent of the lesions was significantly decreased at 3 and 7 days after stroke (Fig. 1A). Moreover, IF analysis using microglial marker Iba-1, astrocyte marker GFAP and neuronal marker NeuN, showed that, compared with the sham group, neurons were significantly reduced, while microglia and astrocytes were significantly activated at 1 day after stroke, and this trend gradually recovered at 3 and 7 days after stroke (Fig. 1B), indicating that the animal model of AIS was successfully established and AIS could promote the inflammatory response and neuronal injury.

PGC-1α is the target gene of miR-126a-5p

In order to further study the molecular mechanism of AIS and neuronal injury, we first analyzed the potential target gene in AIS. The role of PGC-1α has been reported in neurodegenerative diseases such as Parkinson's disease, amyotrophic lateral sclerosis and Alzheimer's disease (Hayakawa et al., 2022). PGC-1α is involved in the pathophysiology of these diseases and up-regulation or down-regulation of PGC-1α expression has a positive or negative impact on the prognosis of the disease (Li et al., 2020). However, the role of PGC-1α in the pathophysiology of AIS remains unclear. Therefore, we examined the PGC-1α expression in the AIS animal model by RT-qPCR. Interestingly, compared with sham group, PGC-1α expression was significantly down-regulated in model group in a time-dependent manner (Fig. 2A). The relationship between PGC-1α and miRNA have rarely been reported in cerebrovascular diseases. In order to further study the mechanism of PGC-1α and miRNA in AIS, firstly, bioinformatics prediction results showed that PGC-1α could be combined with miR-126a-5p. Next, we detected the expression of miR-126a-5p in the AIS animal model by RT-qPCR, compared with sham group, miR-126a-5p expression was significantly up-regulated in the model group (Fig. 2C). At the same time, we detected the expression of circRNA_0000927 in the AIS animal model by RT-qPCR, compared with sham group, circRNA_0000927 expression was significantly down-regulated in the model group (Fig. 2B). The results of PGC-1α and miR-126a-5p showed that they had a negative co-expression correlation and PGC-1α was the target miRNA of miR-126a-5p.

MiR-126a-5p is the target gene of circRNA_0000927

As is known to all, the research of miR-126a-5p focuses on the field of cancer treatment (Wu and Li, 2022), and the research on AIS and neuronal injury is still a blank. In order to further study the molecular mechanism of miR-126a-5p in AIS and neuronal injury, we first analyzed the potential target circRNA binding by miR-126a-5p. Expectedly, bioinformatics prediction results showed that circRNA_0000927 could be combined with miR-126a-5p. At the same time, FISH showed that circRNA_0000927 was in the cytoplasm and cytosol in sham and model groups, therefore, circRNA_0000927 might function as the ceRNA for miR-126a-5p (Fig. 3A). Similarly, further detection of double luciferase reporter assay

confirmed the binding of circRNA RMDN2 to miR-126a-5p (Fig. 3B). Double luciferase reporter was used to confirm the relationship between circRNA_0000927 and miR-126a-5p. Compared with decreased circRNA-WT group, the relative luciferase activity of circRNA-MU reporter was not noticeable changed. The results of circRNA_0000927 and miR-126a-5p showed that they had a negative co-expression correlation. At the same time, further detection of double luciferase reporter assay confirmed the binding of PGC-1α to miR-126a-5p (Fig. 3C). Based on these results, we further speculated that circRNA_0000927 might relieve the AIS and neuronal injury by inhibiting miR-126a-5p expression *in vivo*. At the same time, we speculated that circRNA_0000927 and PGC-1α had a positive co-expression correlation. The results were completely in line with our expectation and circRNA_0000927 would promote the expression of PGC-1α (Fig. 2A, 3B-C), indicating the circRNA_0000927 could promote the neuronal injury and AIS via miR-126a-5p /PGC-1α axis.

AIS could aggravate the inflammasome formation and activate the inflammatory response in the animal model

The NLRP3 inflammasome is consists of ASC, Caspase-1 and NLRP3. After receiving the priming signals, NLRP3 inflammasome activation is induced by pathogen-associated molecular patterns (PAMPs) or damage-associated molecular patterns (DAMPs) (Wu et al., 2015). Oligomerization of NLRP3 structural proteins binds to PYD of the adaptator protein ASC, and then CARD of ASC binds to CARD on pro-Caspase-1 to form an intact and active NLRP3 inflammasome, which promotes self-cleavage of pro-Caspase-1 to produce the active effector protein Caspase-1 (Yang et al., 2022b). Caspase-1 can cleave the GSDMD to release the N-terminal domain of GSDMD. N-GSDMD can bind to phosphatidylserine and phosphoinositol and punch on the cell membrane, leading to the imbalance between the inside and outside of the cell and cell death, causing cell contents release and inflammation (Zemel et al., 2021). In addition to cleaving GSDMD, Caspase-1 can also induce the conversion of IL-1β from immature to active state (Chaube et al., 2015). After cell death, IL-1β will be released out of the cell to induce the neuro-inflammation (Chen et al., 2018). Therefore, inflammatory response and NLRP3 inflammasome can be considered as markers of AIS. Firstly, compared with sham group, the level of IL-1β was also significantly increased in the model group (Fig. 4A). Secondly, compared with sham group, the protein expression of NLRP3, ASC and Caspase-1 was significantly increased in the model group (Fig. 4B-E), indicating that AIS could aggravate the inflammasome formation and activate the inflammatory response in the animal model. Therefore, based on these results, we further speculated that circRNA_0000927 could promote the inflammatory response to neuronal injury via miR-126a-5p/PGC-1α axis in the AIS animal model.

Over-expression of circRNA_0000927 and inhibition of miR-126a-5p relieve the neuronal injury in the hypoxia/reoxygenation cell model

Whether the experimental results *in vitro* are consistent with the AIS animal model is a question we are very concerned about, in order to find out the mystery, we successfully established the primary neuron model with hypoxia/reoxygenation treatment and transfected vector-miR-126a-5p inhibitor and vector-circRNA_0000927 into the hypoxia/reoxygenation cell model. Compared with control and model groups,

the RT-qPCR results indicated that vector-miR-126a-5p inhibitor transfection significantly down-regulated the expression of miR-126a-5p and up-regulated the expression of PGC-1α and vector-circRNA_0000927 over-expression transfection significantly up-regulated the expression of circRNA_0000927 and PGC-1α in the primary neuron (Fig. 5A-C). Furthermore, we detected the expression of IL-1β by ELISA assay. Compared with model group, the level of IL-1β in the vector-miR-126a-5p inhibitor and circRNA_0000927 over-expression groups was significantly decreased (Fig. 5D). Moreover, cell apoptosis was detected using TUNEL assay. Interestingly, compared with model group, less apoptosis cells were observed in vector-miR-126a-5p inhibitor and circRNA_0000927 over-expression groups (Fig. 5E, K). At the same time, compared with model group, the expression of NLRP3, ASC, Caspase-1 was significantly down-regulated and PGC-1α was significantly up-regulated in the vector-miR-126a-5p inhibitor and circRNA_0000927 over-expression groups (Fig. 5F-J), this was consistent with the experimental results of the AIS animal model, indicating that over-expression of circRNA_0000927 and inhibition of miR-126a-5p expression could relieve the neuronal injury in the hypoxia/reoxygenation cell model.

4. Discussion

Stroke refers to the lesion that blood perfusion or oxygen supply is restored to the brain tissue after a period of ischemia, and the damage caused by ischemia to the tissue is not alleviated, and even continues to worsen (Choi et al., 2020). Stroke is the main pathophysiological process of brain dysfunction in most ischemic cerebrovascular diseases. Stroke can be divided into three stages (Nakao et al., 2022): 1) Acute phase: occurs within a few minutes or hours after cerebral ischemia, which is caused by the necrosis of nerve cells and brain tissue injury directly; 2) Subacute phase: occurs several days after brain ischemia, that is, the molecular cell damage stage. Excitatory amino acid toxicity, cell apoptosis, calcium overload, NO toxicity, oxygen radicals, mitochondrial dysfunction and energy metabolism disorders are involved in the brain tissue injury at this stage. 3) Delayed injury period: occurs several days to several weeks after cerebral ischemia, vasogenic edema and a large number of inflammatory reactions occur in the brain tissue, which further aggravate the damage of nerve cells (Eichel et al., 2022). Among them, AIS is the most lethal pathological stage. Therefore, it is of great significance to find effective ways to understand the molecular mechanism for the effective AIS treatment and the neuroprotection of the ischemic brain after stroke.

Until now, circRNA has been recognized as an important type of non-coding RNA, an important regulator of cellular processes, and an active participant in various signal transduction pathways (Bauer et al., 2022). There is increasing evidence that they regulate various cellular functions, such as cell proliferation, cell growth, cell migration, stem cell maintenance, epithelial mesenchymal transformation, and apoptosis (Li et al., 2022). In addition, the study of the interactions between circRNA and other biomolecules, such as lipids and second messengers, will further elucidate the biological functions of circRNA under physiological or pathological conditions. The potential clinical application prospect of circRNA is huge (Liang et al., 2022). CircRNA is often abnormally expressed and expressed in cerebrovascular disease and high tissue specificity (Meng et al., 2022). Therefore, targeted therapy targeting circRNA may be developed into a new way to treat cerebrovascular disease in the future, and theoretically, it may not

cause the harmful side effects to healthy tissues (Miozzo et al., 2022). In the traditional clinical diagnosis and treatment, imaging diagnosis, such as CT, MRI and other technologies as well as the application of disease markers, for the diagnosis and treatment of AIS patients provide a certain guiding role (Nichols et al., 2018). However, traditional examination still have great limitations in accurately predicting the occurrence and development of diseases. CircRNA is widespread and relatively stable in organisms, and can be detected in body fluids such as blood and urine, so it has the possibility of being used as a clinical marker (Rog-Zielinska et al., 2015). In addition, the novel studies showed that circRNAs can bind specific target genes and regulate their functions, thus affecting the occurrence and progression of diseases.

In this study, based on bioinformatics prediction, we screened out several circRNAs that were differentially expressed in AIS, among which the most significant circRNA was circRNA_0000927. To study the function of circRNA_0000927. Next, we used bioinformatics database to construct the interaction network between circRNA and miRNA. At this point, we basically determined that circRNA_0000927 may play an important biological role in the occurrence and development of AIS. To verify our prediction, we performed the RT-qPCR in AIS animal model, and the results showed that circRNA_0000927 was significantly down-regulated in the AIS animal model, so it is reasonable to believe that our study is of great significance. So far, many literatures have reported that circRNA_0000927 plays an important role in a variety of tumors (Zhang et al., 2022), but the role of circRNA_0000927 in AIS is still unsolved. Our study found that the expression of circRNA_0000927 was significantly decreased in the AIS animal model, and circRNA_0000927 could promote the development and deterioration of AIS by binding to target miRNA. The mechanism of circRNA_0000927 is not yet fully understood, but our study suggests that circRNA RMDN2 has the potential to inhibit and mitigate the occurrence and development of AIS and may be a novel therapeutic target for AIS.

MiR-126a-5p, as a novel member of the miRNA family, has been found to be involved in traumatic fractures of the brain, tumors, osteoarthritis, endothelial cell injury of coronary heart disease, myocardial cell fibrosis and other aspects (Yu et al., 2022). However, the role of miR-126a-5p in AIS and neuronal injury has not been reported. In this study, we confirmed that miR-126a-5p was up-regulated in the process of AIS in animal model, and bioinformatics also predicted that miR-126a-5p, as a target gene of circRNA_0000927, was involved in the regulation of the development of AIS. After transfection with miR-126a-5p inhibitor and over-expresson circRNA_0000927 vectors, it was found that the expression of NLRP3, ASC, Caspase-1 and PGC-1α was decreased after miR-126a-5p inhibition and over-expresson circRNA_0000927. At the same time, after miR-126a-5p was inhibited, the survival rate of primary neurons was increased and the apoptosis rate of primary neurons was decreased. Therefore, our experiment confirmed that miR-126a-5p plays a crucial role in the process of AIS, and the promotion of miR-126a-5p on AIS may be realized by regulating the effect of primary neurons apoptosis.

Previous studies found that PGC-1α had protective effects in primary neurons and human astrocytes cultured *in vitro* (Yang et al., 2022c; Yoshida and Ohki, 2020). Over-expression of PGC-1α in neurons could inhibit the neuronal apoptosis, while inhibition of PGC-1α expression could induce the neuronal apoptosis (Yang et al., 2022b). It was found that the expression of PGC-1α and related antioxidant components

were increased in AIS patients, and the increased level of PGC-1α was mainly located in activated astrocytes (Wu and Li, 2022; Wu et al., 2015). By over-expressing PGC-1α in astrocytes *in vitro*, ROS levels were reduced, pro-inflammatory factor release was reduced, and neuronal activity was ultimately improved. These results suggested that PGC-1α in astrocytes might act as an endogenous protective mechanism in AIS patients (Tu et al., 2021). PGC-1α is also involved in regulating the glutathione system of astrocytes, which in turn reduces the oxidative and metabolic damage (Stern et al., 2022). Considering these neuroprotective effects of PGC-1α, regulating the level of PGC-1α could be a promising neuro-protective strategy (Savini et al., 2022). In this study, we reported the previously unknown specific role of circRNA_0000927-miR-126a-5p-PGC-1α axis in the pathophysiology of AIS, which could provide a new theoretical basis for revealing the molecular mechanism of neuro-protection of PGC-1α.

5. Conclusion

In summary, vital circRNA_0000927 is down-regulated in AIS animal model and is related to prediction and treatment of the occurrence and development of AIS. CircRNA_0000927 promotes the AIS occurrence and deterioration and neuronal injury by targeting the miR-126a-5p and PGC-1α and activating the inflammatory response.

Abbreviations

AIS: acute ischemic stroke; CNS: central nervous system; miRNA: microRNA; PGC-1α: peroxisome proliferator-activated receptor-γ co-activator-1α; PFA: paraformaldehyde; HE: Hematoxylin-eosin; FBS: fetal bovine serum; IF: immunofluorescence; FISH: fluorescence in situ hybridization; PAMPs: pathogen-associated molecular patterns; DAMPs: damage-associated molecular patterns

Declarations

1) Ethical Approval and Consent to participate

This article contains any studies with animals performed by any of the authors.

The experimental mice followed the regulations of the Experimental Animal Ethics Committee of First Teaching Hospital of Tianjin University of Traditional Chinese Medicine (Approval NO. IRM-DWLL-2021167).

2) Consent for publication

This manuscript has not been published in whole or in part and is not being considered for publication elsewhere. This manuscript does not violate or infringe upon any existing copyright/s license/s from any third party. All authors agreed to the publication of the manuscript.

3) Availability of data and materials

The data and materials involved in this manuscript were original results. If the magazine or readers need the data and materials, we can also upload all the data and materials to provide online.

4) Competing interest

This manuscript has not been published in whole or in part and is not being considered for publication elsewhere. This manuscript does not violate or infringe upon any existing copyright/s license/s from any third party. All authors contributed significantly to work and agree with the manuscript's content. There are no conflicts of interest.

5) Funding

This work was financially supported by the National Natural Science Foundation (NO.81704148).

6) Authors' contributions

Meng Wang: Methodology, Writing-original draft. Hong Li: Methodology, Data curation, Validation. Yulin Qian: Methodology, Visualization. Shanshan Zhao: Investigation, Validation, Formal analysis. Hao Wang and Yu Wang: Resources. Tao Yu: Conceptualization, Writing-original draft, Writing- review & editing.

7) Acknowledgments

This work was financially supported by the National Natural Science Foundation (NO.81704148).

References

1. Baldelli S, Aquilano K, Ciriolo MR. PGC-1alpha buffers ROS-mediated removal of mitochondria during myogenesis. Cell Death Dis. 2014;5:e1515.
2. Bauer KE, Bargenda N, Schieweck R, Illig C, Segura I, Harner M, Kiebler MA. RNA supply drives physiological granule assembly in neurons. Nat Commun. 2022;13(1):2781.
3. Brancaccio P, Anzilotti S, Cuomo O, Vinciguerra A, Campanile M, Herchuelz A, Amoroso S, Annunziato L, Pignataro G. Preconditioning in hypoxic-ischemic neonate mice triggers Na(+)-Ca(2+) exchanger-dependent neurogenesis. Cell Death Discov. 2022;8(1):318.
4. Chaube B, Malvi P, Singh SV, Mohammad N, Viollet B, Bhat MK. 2015. AMPK maintains energy homeostasis and survival in cancer cells via regulating p38/PGC-1α-mediated mitochondrial biogenesis. Cell Death Discovery 1(1).
5. Chen D, Dixon BJ, Doycheva DM, Li B, Zhang Y, Hu Q, He Y, Guo Z, Nowrangi D, Flores J, Filippov V, Zhang JH, Tang J. IRE1alpha inhibition decreased TXNIP/NLRP3 inflammasome activation through miR-17-5p after neonatal hypoxic-ischemic brain injury in rats. J Neuroinflammation. 2018;15(1):32.
6. Choi KJ, Nam JK, Kim JH, Choi SH, Lee YJ. Endothelial-to-mesenchymal transition in anticancer therapy and normal tissue damage. Exp Mol Med. 2020;52(5):781–92.

7. De Vitto H, Bode AM, Dong Z. The PGC-1/ERR network and its role in precision oncology. NPJ Precis Oncol. 2019;3:9.
8. Eichel K, Uenaka T, Belapurkar V, Lu R, Cheng S, Pak JS, Taylor CA, Südhof TC, Malenka R, Wernig M, Özkan E, Perrais D, Shen K. 2022. Endocytosis in the axon initial segment maintains neuronal polarity. Nature.
9. Guida MC, Birse RT, Dall'Agnese A, Toto PC, Diop SB, Mai A, Adams PD, Puri PL, Bodmer R. Intergenerational inheritance of high fat diet-induced cardiac lipotoxicity in Drosophila. Nat Commun. 2019;10(1):193.
10. Hayakawa E, Guzman C, Horiguchi O, Kawano C, Shiraishi A, Mohri K, Lin MF, Nakamura R, Nakamura R, Kawai E, Komoto S, Jokura K, Shiba K, Shigenobu S, Satake H, Inaba K, Watanabe H. Mass spectrometry of short peptides reveals common features of metazoan peptidergic neurons. Nat Ecol Evol; 2022.
11. Hellwig L, Brada M, Held U, Hagmann C, Bode P, Frontzek K, Frey B, Brotschi B, Grass B. Association of perinatal sentinel events, placental pathology and cerebral MRI in neonates with hypoxic-ischemic encephalopathy receiving therapeutic hypothermia. J Perinatol. 2022;42(7):885–91.
12. Li G, Ma L, He S, Luo R, Wang B, Zhang W, Song Y, Liao Z, Ke W, Xiang Q, Feng X, Wu X, Zhang Y, Wang K, Yang C. Author Correction: WTAP-mediated m(6)A modification of lncRNA NORAD promotes intervertebral disc degeneration. Nat Commun. 2022;13(1):3572.
13. Li T, Li K, Zhang S, Wang Y, Xu Y, Cronin SJF, Sun Y, Zhang Y, Xie C, Rodriguez J, Zhou K, Hagberg H, Mallard C, Wang X, Penninger JM, Kroemer G, Blomgren K, Zhu C. Overexpression of apoptosis inducing factor aggravates hypoxic-ischemic brain injury in neonatal mice. Cell Death Dis. 2020;11(1):77.
14. Liang YL, Zhang Y, Tan XR, Qiao H, Liu SR, Tang LL, Mao YP, Chen L, Li WF, Zhou GQ, Zhao Y, Li JY, Li Q, Huang SY, Gong S, Zheng ZQ, Li ZX, Sun Y, Jiang W, Ma J, Li YQ, Liu N. A lncRNA signature associated with tumor immune heterogeneity predicts distant metastasis in locoregionally advanced nasopharyngeal carcinoma. Nat Commun. 2022;13(1):2996.
15. Meng X, Peng J, Xie X, Yu F, Wang W, Pan Q, Jin H, Huang X, Yu H, Li S, Feng D, Liu Q, Fang L, Lee MH. Roles of lncRNA LVBU in regulating urea cycle/polyamine synthesis axis to promote colorectal carcinoma progression. Oncogene; 2022.
16. Miozzo F, Valencia-Alarcon EP, Stickley L, Majcin Dorcikova M, Petrelli F, Tas D, Loncle N, Nikonenko I, Dib B, P. and Nagoshi E. Maintenance of mitochondrial integrity in midbrain dopaminergic neurons governed by a conserved developmental transcription factor. Nat Commun. 2022;13(1):1426.
17. Nakao Y, Nakamura S, Htun Y, Mitsuie T, Koyano K, Ohta K, Konishi Y, Miki T, Ueno M, Kusaka T. Cerebral hemodynamic response during the resuscitation period after hypoxic-ischemic insult predicts brain injury on day 5 after insult in newborn piglets. Sci Rep. 2022;12(1):13157.
18. Nichols M, Pavlov EV, Robertson GS. Tamoxifen-induced knockdown of the mitochondrial calcium uniporter in Thy1-expressing neurons protects mice from hypoxic/ischemic brain injury. Cell Death Dis. 2018;9(6):606.

19. Presslauer C, Bizuayehu T, Kopp T, Fernandes M, J.M. and Babiak I. Dynamics of miRNA transcriptome during gonadal development of zebrafish. Sci Rep. 2017;7:43850.
20. Rog-Zielinska EA, Craig MA, Manning JR, Richardson RV, Gowans GJ, Dunbar DR, Gharbi K, Kenyon CJ, Holmes MC, Hardie DG, Smith GL, Chapman KE. Glucocorticoids promote structural and functional maturation of foetal cardiomyocytes: a role for PGC-1alpha. Cell Death Differ. 2015;22(7):1106–16.
21. Savini M, Folick A, Lee YT, Jin F, Cuevas A, Tillman MC, Duffy JD, Zhao Q, Neve IA, Hu PW, Yu Y, Zhang Q, Ye Y, Mair WB, Wang J, Han L, Ortlund EA, Wang MC. Lysosome lipid signalling from the periphery to neurons regulates longevity. Nat Cell Biol. 2022;24(6):906–16.
22. Siegerist F, Lange T, Iervolino A, Koppe TM, Zhou W, Capasso G, Endlich K, Endlich N. Evaluation of endogenous miRNA reference genes across different zebrafish strains, developmental stages and kidney disease models. Sci Rep. 2021;11(1):22894.
23. Song YX, Sun JX, Zhao JH, Yang YC, Shi JX, Wu ZH, Chen XW, Gao P, Miao ZF, Wang ZN. Non-coding RNAs participate in the regulatory network of CLDN4 via ceRNA mediated miRNA evasion. Nat Commun. 2017;8(1):289.
24. Song YX, Sun JX, Zhao JH, Yang YC, Shi JX, Wu ZH, Chen XW, Gao P, Miao ZF, Wang ZN. Author Correction: Non-coding RNAs participate in the regulatory network of CLDN4 via ceRNA mediated miRNA evasion. Nat Commun. 2021;12(1):3149.
25. Stern S, Lau S, Manole A, Rosh I, Percia MM, Ben Ezer R, Shokhirev MN, Qiu F, Schafer S, Mansour AA, Mangan KP, Stern T, Ofer P, Stern Y, Mendes D, Djamus AP, Moore J, Nayak LR, Laufer R, Aicher SH, Rhee A, Wong A, Nguyen TL, Linker T, Winner SB, Freitas B, Jones BC, Sagi E, Bardy I, Brice C, Winkler A, Marchetto J, M.C. and Gage FH. Reduced synaptic activity and dysregulated extracellular matrix pathways in midbrain neurons from Parkinson's disease patients. NPJ Parkinsons Dis. 2022;8(1):103.
26. Tarocco A, Morciano G, Perrone M, Cafolla C, Ferre C, Vacca T, Pistocchi G, Meneghin F, Cocchi I, Lista G, Cetin I, Greco P, Garani G, Stella M, Natile M, Ancora G, Savarese I, Campi F, Bersani I, Dotta A, Tiberi E, Vento G, Chiodin E, Staffler A, Maranella E, Di Fabio S, Wieckowski MR, Giorgi C, Pinton P. Increase of Parkin and ATG5 plasmatic levels following perinatal hypoxic-ischemic encephalopathy. Sci Rep. 2022;12(1):7795.
27. Tu YF, Jiang ST, Chiang CW, Chen LC, Huang CC. Endothelial-specific insulin receptor substrate-1 overexpression worsens neonatal hypoxic-ischemic brain injury via mTOR-mediated tight junction disassembly. Cell Death Discov. 2021;7(1):150.
28. Wu F, Li C. KLF2 up-regulates IRF4/HDAC7 to protect neonatal rats from hypoxic-ischemic brain damage. Cell Death Discov. 2022;8(1):41.
29. Wu SP, Kao CY, Wang L, Creighton CJ, Yang J, Donti TR, Harmancey R, Vasquez HG, Graham BH, Bellen HJ, Taegtmeyer H, Chang CP, Tsai MJ, Tsai SY. Increased COUP-TFII expression in adult hearts induces mitochondrial dysfunction resulting in heart failure. Nat Commun. 2015;6:8245.

30. Xu J, Xu J, Liu X, Jiang J. The role of lncRNA-mediated ceRNA regulatory networks in pancreatic cancer. Cell Death Discov. 2022;8(1):287.
31. Yang J, Qi M, Fei X, Wang X, Wang K. Hsa_circRNA_0088036 acts as a ceRNA to promote bladder cancer progression by sponging miR-140-3p. Cell Death Dis. 2022a;13(4):322.
32. Yang L, Ball A, Liu J, Jain T, Li YM, Akhter F, Zhu D, Wang J. Cyclic microchip assay for measurement of hundreds of functional proteins in single neurons. Nat Commun. 2022b;13(1):3548.
33. Yang L, Yu X, Zhang Y, Liu N, Xue X, Fu J. Caffeine treatment started before injury reduces hypoxic-ischemic white-matter damage in neonatal rats by regulating phenotypic microglia polarization. Pediatr Res; 2022c.
34. Yao T, Vanduffel W. Neuronal congruency effects in macaque prefrontal cortex. Nat Commun. 2022;13(1):4702.
35. Yoshida T, Ohki K. Natural images are reliably represented by sparse and variable populations of neurons in visual cortex. Nat Commun. 2020;11(1):872.
36. Yu J, Loh K, Yang HQ, Du MR, Wu YX, Liao ZY, Guo A, Yang YF, Chen B, Zhao YX, Chen JL, Zhou J, Sun Y, Xiao Q. The Whole-transcriptome Landscape of Diabetes-related Sarcopenia Reveals the Specific Function of Novel lncRNA Gm20743. Commun Biol. 2022;5(1):774.
37. Zemel BM, Nevue AA, Dagostin A, Lovell PV, Mello CV, von Gersdorff H. Resurgent Na(+) currents promote ultrafast spiking in projection neurons that drive fine motor control. Nat Commun. 2021;12(1):6762.
38. Zhang Y, Luo M, Cui X, O'Connell D, Yang Y. Long noncoding RNA NEAT1 promotes ferroptosis by modulating the miR-362-3p/MIOX axis as a ceRNA. Cell Death Differ; 2022.
39. Zhang Y, Xu N, Ding Y, Doycheva DM, Zhang Y, Li Q, Flores J, Haghighiabyaneh M, Tang J, Zhang JH. Chemerin reverses neurological impairments and ameliorates neuronal apoptosis through ChemR23/CAMKK2/AMPK pathway in neonatal hypoxic-ischemic encephalopathy. Cell Death Dis. 2019;10(2):97.
40. Zhang ZB, Xiong LL, Xue LL, Deng YP, Du RL, Hu Q, Xu Y, Yang SJ, Wang TH. MiR-127-3p targeting CISD1 regulates autophagy in hypoxic-ischemic cortex. Cell Death Dis. 2021;12(3):279.
41. Zhu X, Yan J, Bregere C, Zelmer A, Goerne T, Kapfhammer JP, Guzman R, Wellmann S. RBM3 promotes neurogenesis in a niche-dependent manner via IMP2-IGF2 signaling pathway after hypoxic-ischemic brain injury. Nat Commun. 2019;10(1):3983.

Figures

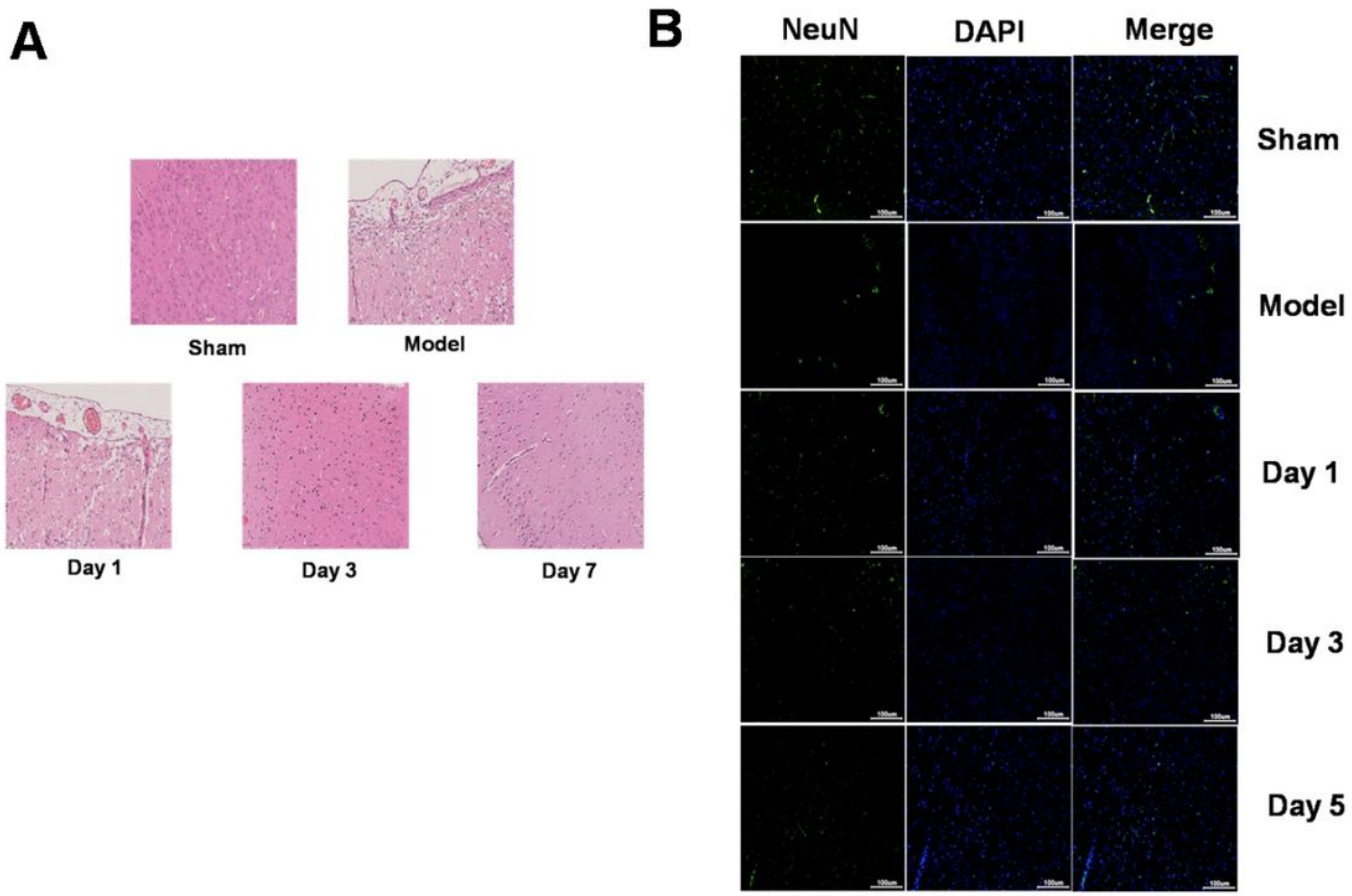

Figure 1

The animal model of AIS is successfully established. (A) HE staining of brain tissues in sham and model groups; (B) IF staining of microglia, astrocyte and neuron in sham and model groups. All data were expressed as mean ± standard deviation, **P*<0.05, ***P*<0.01, *** *P*<0.001 *vs.* sham group.

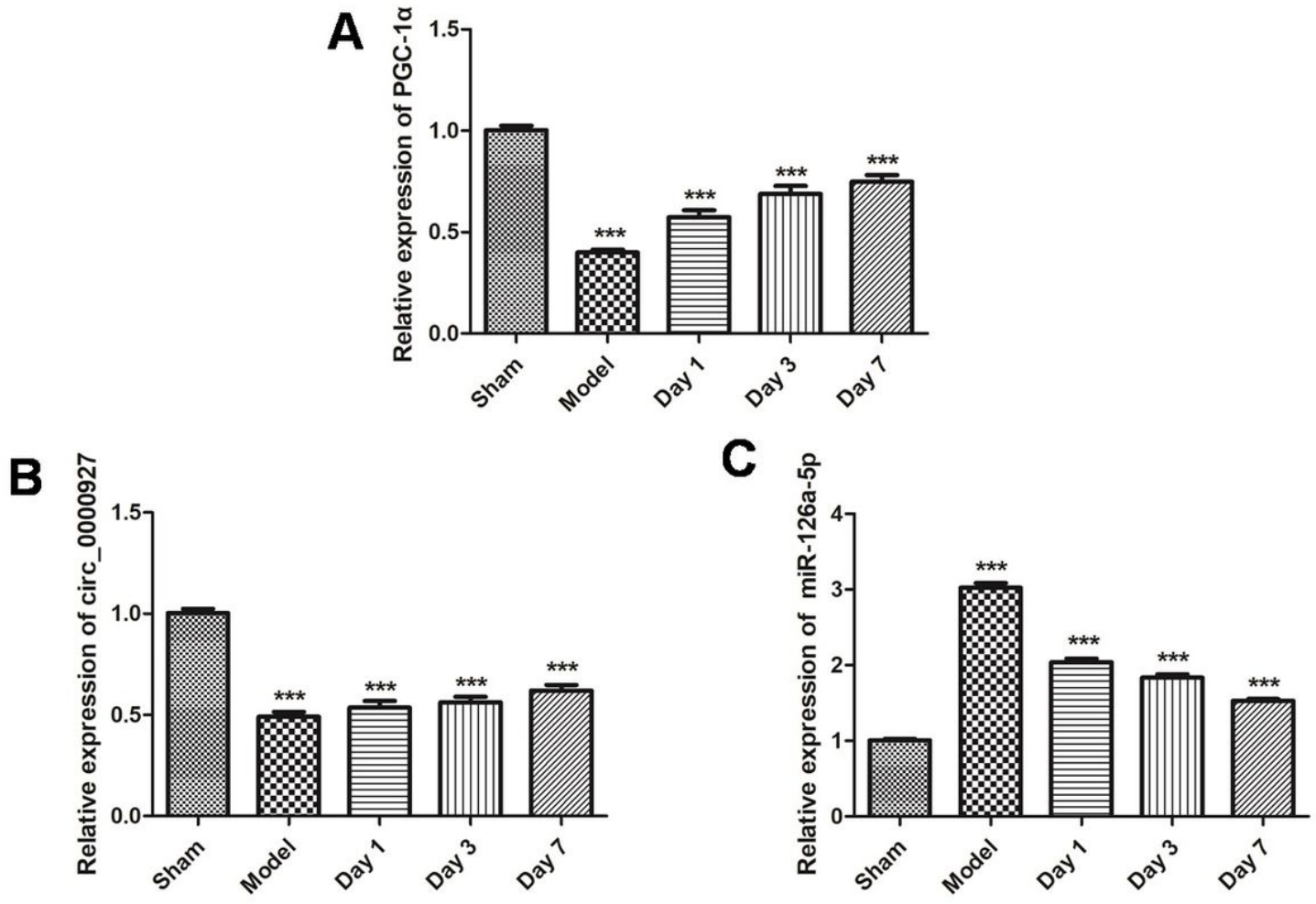

Figure 2

PGC-1α is the target gene of miR-126a-5p. (A) PGC-1α expression level was detected in sham and model groups; (B) CircRNA_0000927 expression level was detected in sham and model groups; (C) MiR-126a-5p expression level was detected in sham and model groups; All data were expressed as mean ± standard deviation, **P*<0.05, ***P*<0.01, *** *P*<0.001 *vs.* sham group.

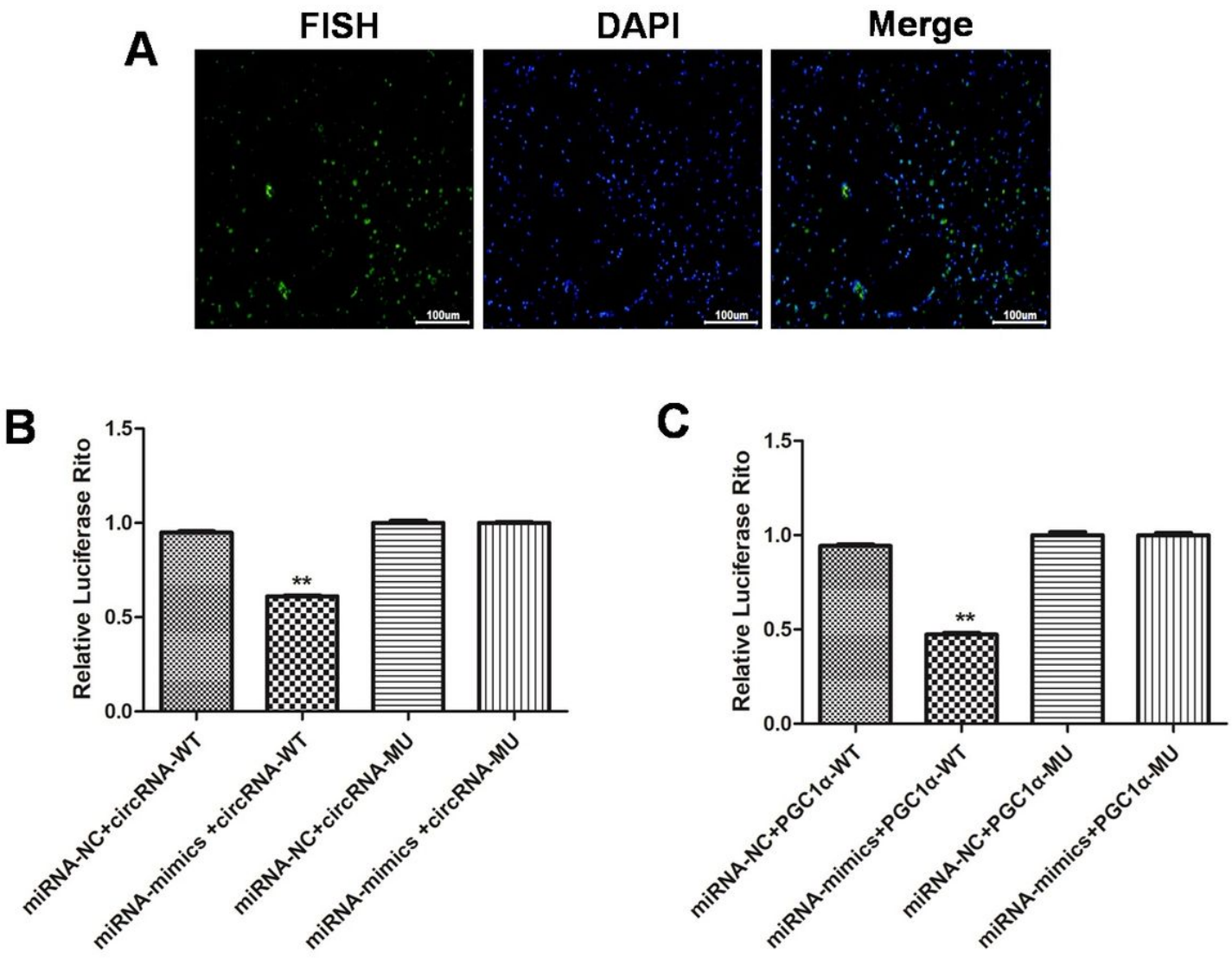

Figure 3

MiR-126a-5p is the target gene of circRNA_0000927. (A) CircRNA_0000927 localization was detected in sham and model groups. (B) Double luciferase reporter detected circRNA_0000927 binding to miR-126a-5p in model group; (C) Double luciferase reporter detected PGC-1α binding to miR-126a-5p in model group; All data were expressed as mean ± standard deviation, **P*<0.05, ***P*<0.01, *** *P*<0.001 *vs.* sham group.

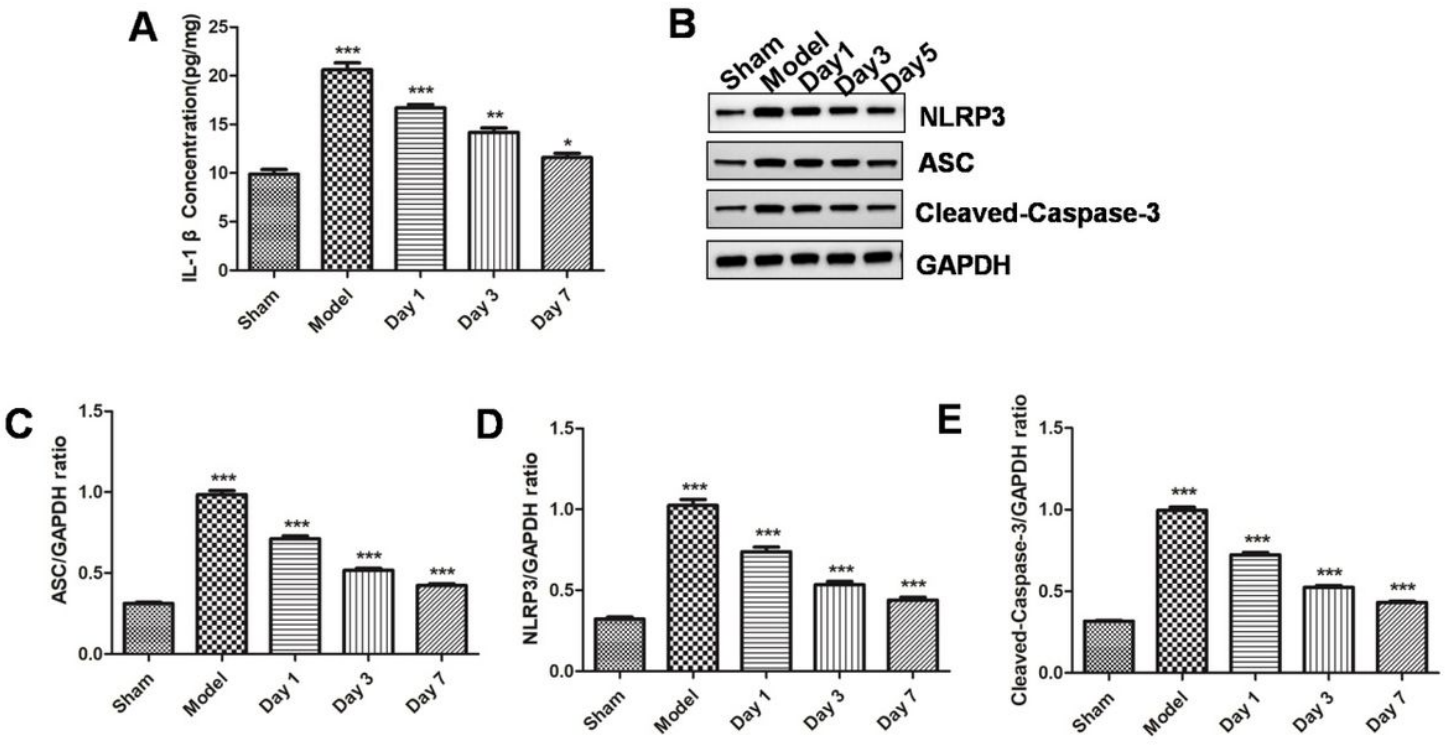

Figure 4

AIS could aggravate the inflammasome formation and activate the inflammatory response in the animal model. (A) Detection of IL-1β levels in different groups; (B-E) NLRP3, ASC and Caspase-1 protein expression level was detected in different groups. All data were expressed as mean ± standard deviation, **P*<0.05, ***P*<0.01, *** *P*<0.001 *vs.* sham group.

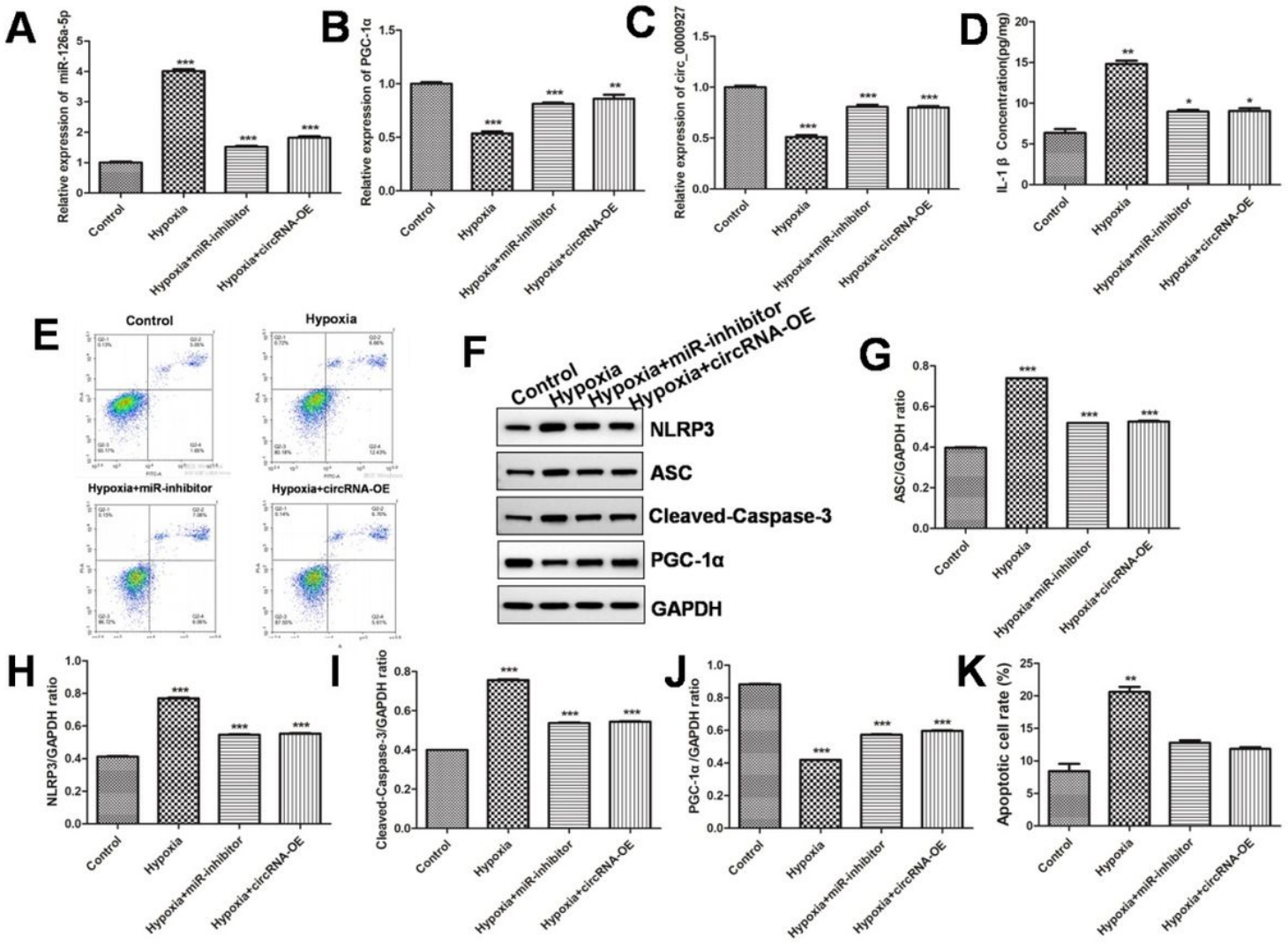

Figure 5

Over-expression of circRNA_0000927 and inhibition of miR-126a-5p relieve the neuronal injury in the hypoxia/reoxygenation cell model. (A-C) Detection of vector-miR-126a-5p inhibitor and circRNA_0000927 over-expression vectors transfection efficiency in the hypoxia/reoxygenation cell model; (D) Detection of IL-1β levels in the hypoxia/reoxygenation cell model; (E,K) Neuron apoptosis was detected by TUNEL staining in the hypoxia/reoxygenation cell model;; (F-J) NLRP3, ASC, Caspase-1 and PGC-1α expression level was detected in the hypoxia/reoxygenation cell model. All data were expressed as mean ± standard deviation, **P*<0.05, ***P*<0.01, *** *P*<0.001 *vs.* control group.

Supplementary Files

This is a list of supplementary files associated with this preprint. Click to download.

- Supplementaryfiles.docx